Proceedings of the ASME 2015 International Design Engineering Technical Conferences & Computers and Information in Engineering Conference
IDETC/CIE 2015
August 2-5, 2015, Boston, Massachusetts, USA

DETC2015-47863

FLEXURE DESIGN FOR EIGHT-BAR RECTILINEAR MOTION MECHANISM

Yang Liu
Robotics and Automation Laboratory
Department of Mechanical and Aerospace Engineering
University of California
Irvine, California 92697
Email: liuy14@uci.edu

J. Michael McCarthy*
Robotics and Automation Laboratory
Department of Mechanical and Aerospace Engineering
University of California
Irvine, California 92697
Email: jmmccart@uci.edu

ABSTRACT

This paper replaces the hinged pivots of an eight-bar linkage with flexure joints in order to achieve a flexure-connected linkage system that guides rectilinear movement of its end-effector. The goal is a linkage design that can be reduced in size to provide a suspension for the proof masses of a MEMS gyroscope. The symmetric design of the linkage and its long travel relative to other MEMS suspensions has the potential to provide a number of advantages, such as the reduction of quadrature error. The design presented yields 0.1% deviation over its range of movement. An example also presents the driving linkage of the MEMS gyroscope, which is also designed as flexure connected linkage.

INTRODUCTION

This paper presents an eight-bar linkage in which the hinged pivots have been replaced by flexures in order to guide the rectilinear movement of a MEMS gyroscope. The flexure-connected eight-bar linkage provides a long-travel rectilinear suspension for the proof masses in the MEMS gyroscope, which reduces quadrature error.

Existing rectilinear motion linkages have 10 bars, see Kempe (1877) [4]. Our goal is an eight-bar linkage that guides rectilinear movement with low error and with no link overlap so the hinged joints can be replaced with flexures. A flexure allows movement through bending of its elements. An example of application of flexure pivots can be seen from a 2-DOF flexure parallel mechanism [1].

The resulting flexure-connected eight-bar linkage has dimensions of approximately $200mm \times 150mm$ and provides 33mm rectilinear movement with a maximum deviation of 0.1%.

LITERATURE REVIEW

Suspensions for MEMS gyroscope are usually formed from springs, such as the *Crab-leg spring, U-spring, Serpentine spring and Folded-flexure spring* (2006) [2]. These suspensions are asymmetric, which introduces in quadrature error. Shi et al. (2006) [2] provide design principles to reduce quadrature error.

Our research provides another approach by designing a symmetric eight-bar and introducing flexures as the pivots, in order to obtain a compliant mechanism that provides a rectilinear movement. The symmetric structure of this suspension results in high-rate sensitivity and low temperature dependent drift [3]. In addition, it provides a long travel rectilinear movement of the proof mass.

The synthesis of an eight-bar linkage to reach five task positions has been presented by Soh and McCarthy (2007) [6] and Sonawale and McCarthy (2014) [9]. This method starts from two 3R chain robots and by adding two RR constraints to get one degree-of-freedom eight-bar linkage. In this research, we follow this procedure and obtain a number of eight-bar linkages from which we chose the designs with non-overlapping links. This provides a simple way to introduce flexures into the linkage.

Eight-bar linkages that have pivots replaced by flexures are

*Address all correspondence to this author.

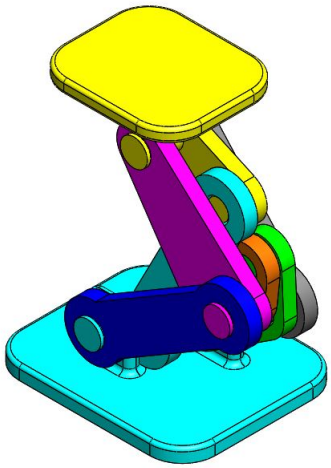

FIGURE 1. AN EXAMPLE OF A RECTILINEAR EIGHT-BAR LINKAGE WITH OVERLAPPING LINKS.

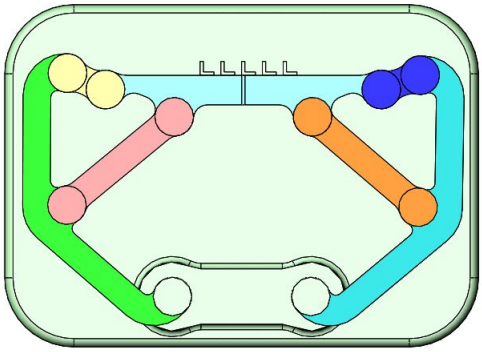

FIGURE 2. A SYMMETRIC RECTILINEAR EIGHT-BAR LINKAGE WITH NON-OVERLAPPING LINKS.

examples of compliant mechanisms. Compliant mechanisms have proven to have a wide range of applications both in MEMS devices and larger scale systems, [11] [10]. Howell [12, 14] presents the design rules for the introduction of flexures in traditional pivoted linkage systems. The analysis of beam flexure performance had been presented by Awtar and Slocum (2007) [13]. In this paper, we replace the hinges in our eight-bar linkage design with long-thin beam flexures, analyze the resulting system, and adjust the flexure dimensions to ensure performance.

RECTILINEAR EIGHT-BAR LINKAGE

The method of synthesis of eight-bar linkages start from defining two 3R chain firstly and adding a RR chain constraint after, has already been presented by Soh and McCarthy (2007) [6]. Continuing research on finding all possible ways of applying the RR constraint was presented by Sonawale and McCarthy (2014) [9]. In our research, we specified the five task positions on a straight line. We followed the same procedure to get a number of eight-bar linkages.

Firstly we need to derive the kinematic equations of the planar 3R chain. Let [D] denote the homogeneous transformation from task frame to fixed frame. [G] is the transformation matrix from the 3R chain base to fixed frame. We define [H] as the transformation matrix from task frame to end-effector frame. The length of the 3 moving links were represented as a_1, a_2 and a_3 respectively. θ_1, θ_2 and θ_3 are relative rotation angles of each moving frame. Let Z denote the homogeneous transformation matrix of the moving frame. The homogeneous transformation matrix [D] can be denoted as

$$[D] = [G]Z(\theta_1, 0)Z(\theta_2, a_1)Z(\theta_3, a_2)[H]. \quad (1)$$

Five task positions have already been specified on a straight line so we can solve $(\theta_{1j}, \theta_{2j}, \theta_{3j}), j = 1, ..., 5$ for each of the five task positions using

$$[D_j] = [G]Z(\theta_{1j}, 0)Z(\theta_{2j}, a_1)Z(\theta_{3j}, a_2)[H], \quad j = 1, ..., 5. \quad (2)$$

The next step is defining two RR constraints between any two of the moving link. Let's define $[B_{lj}]$ to be the homogeneous transformation matrix of the l*th* moving link to the fixed frame and $[B_{kj}]$ to be the homogeneous transformation matrix of the k*th* moving link to the fixed frame. The l*th* moving link and the k*th* moving link are connected by a RR constraint link. The joint position, g, is where the RR constraint link connected the l*th* link measured in moving frame $[B_{lj}]$ and w is the joint position where RR constraint link connected the k*th* link measured in moving frame $[B_{kj}]$. In the process of the task frame moving through all the five task positions, the coordinates of two ends of the RR constraint link, measured in the fixed frame, are given by

$$G^j = [B_{lj}]g \quad and \quad W^j = [B_{kj}]w. \quad (3)$$

Relative displacement is introduced for convenient calculation

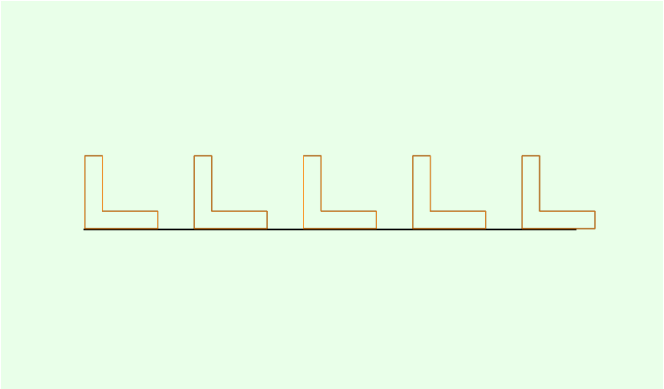

FIGURE 3. TRACING THE END-EFFECTOR PATH OF SYMMETRIC EIGHT-BAR LINKAGE.

$$[R_{1j}] = [B_{lj}][B_{l1}]^{-1} \quad and \quad [S_{1j}] = [B_{kj}][B_{k1}]^{-1}. \tag{4}$$

Substitute equation (4) into equation (3) we get

$$G^j = [R_{1j}]G^1 \quad and \quad W^j = [S_{1j}]W^1. \tag{5}$$

Note that $[R_{11}] = [S_{11}] = [I]$ are identity matrix. The two ends of the RR constraint link were defined by G^j and W^j. Assuming the length of the RR constraint link is R so we can get constraint equations for five take positions

$$([R_{1j}]G^1 - [S_{1j}]W^1]) \cdot ([R_{1j}]G^1 - [S_{1j}]W^1]) = R^2, \quad j = 1,...,5. \tag{6}$$

Here we get five constraint equations and five variables. We can solve for $G^1 = (u,v,1)^T$, $W^1 = (x,y,1)^T$ and R using the five task positions which have been specified on a straight line. The method of solving RR constraint equations of a four-bar linkage has been presented by McCarthy [5]. We used the same method here, subtracting the first of the five equations from the remaining four to reduce the total variables to four. By using Mathematica's *Nsolve* function, we can get all the possible eight-bar linkage designs satisfying our task position requirements.

MEMS IMPLEMENTATION

MEMS fabrication requires single layer design. First, we need to find non-overlap eight-bar linkages from the numerous solutions we obtained from the above synthesis process. This requires all links of the eight-bar linkage must not overlap each other when the end-effector moves through all the five task positions. Here are two examples of overlap and non-overlap eight-bar linkages. The eight-bar linkage shown in Fig.1 is in overlap form. It can provide rectilinear motion but several links have to be placed on different layers to make the whole mechanism work. The one shown in Fig.2 is an example of non-overlap linkage.

The ones we obtained from the synthesis of eight-bar linkages are all in asymmetric shape. We redesigned the eight-bar

TABLE 1. COORDINATES OF TRACING POINTS.

X(mm)	Y(mm)	Z(mm)
34.93411	-70.0572	21.11394
34.94115	-70.0572	21.11394
34.96226	-70.0572	21.11394
34.9974	-70.0571	21.11394
35.04651	-70.057	21.11394
35.10951	-70.0569	21.11394
35.18629	-70.0567	21.11394
35.27672	-70.0566	21.11394
35.38065	-70.0563	21.11394
35.4979	-70.0561	21.11394
35.62828	-70.0558	21.11394
35.77158	-70.0556	21.11394

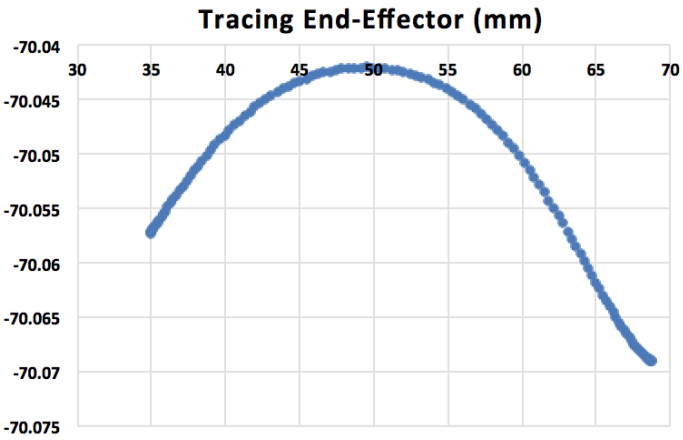

FIGURE 4. THE VERTICAL DEVIATION IS 0.03MM FOR A TRAVEL OF 30MM, WHICH IS 0.1% DEVIATION.

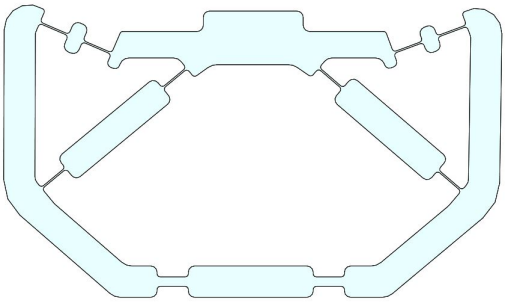

FIGURE 5. THE SYMMETRIC RECTILINEAR EIGHT-BAR LINKAGE WITH HINGES REPLACED WITH BEAM FLEXURES (FLEXURE SUSPENSION).

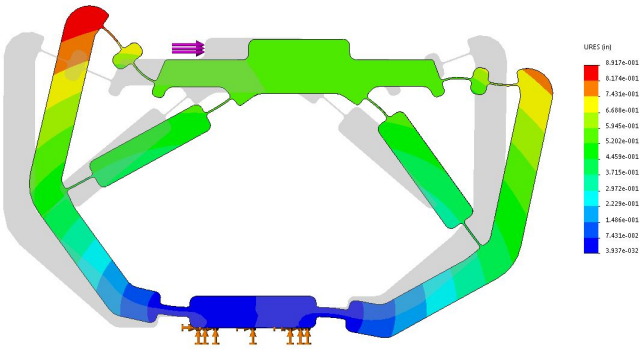

FIGURE 7. FINITE ELEMENT ANALYSIS SHOWING DISPLACEMENTS IN THE EIGHT-BAR FELXURE SUSPENSION.

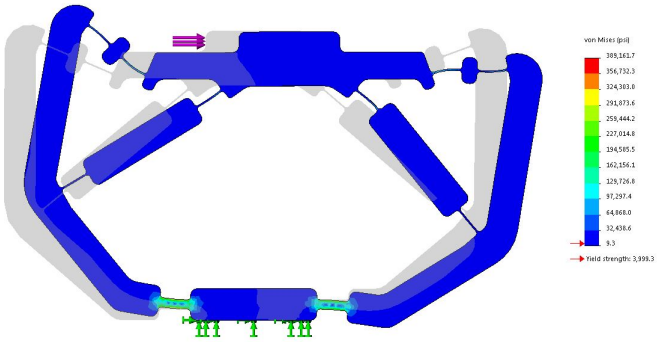

FIGURE 6. FINITE ELEMENT ANALYSIS SHOWING STRESSES IN THE EIGHT-BAR FLEXURE SUSPENSION.

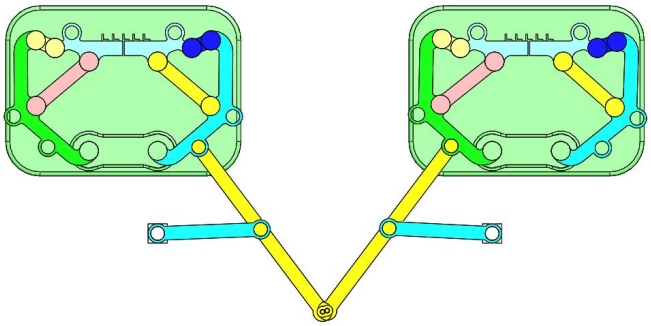

FIGURE 8. DESIGN OF A DRIVING LINKAGE FOR TWO EIGHT-BAR RECTILINEAR MOTION LINKAGES.

linkage and made it perfectly symmetric due to the powerful advantages offered by symmetric shape in MEMS gyroscope application. The redesigned eight-bar linkage is shown in Fig.2.

After redesigning, the end effector still showed very good rectilinear property. After evaluating the rectilinear performance of the symmetric eight-bar linkage, we traced the motion path of the end-effector. The path can be seen in Fig.3, which is a perfect straight line just from observation. We extracted 253 points from the straight line and got the exact coordinates for each point. Part of the points coordinates are shown in Table.1 as an example. A curve shown in Fig.4 was created to show the 253 points. The X-axis and Y-axis represented the X coordinates and Y coordinates of each point. The total displacement in X-direction for the end-effector moved from the first task position to the fifth task position is 33.1 millimeters. During this process, the maximum and minimum Y coordinates of the tracing point were -70.042 millimeters and -70.069 millimeters respectively. The maximum deviation in the Y-direction of the end effector was only 0.027 millimeter while it went horizontally 33.1 millimeters. Here we analyzed the performance of the symmetric eight-bar linkage using millimeter units. We need to scale it to micron units during fabrication. We can see the redesigned symmetric eight-bar linkage manifested perfectly rectilinear motion property.

The next step was replacing all the rigid-body joints with flexure pivots. We used Finite-Element-Analysis method to evaluate the performance of the eight-bar flexure suspension designed before. It turned out that the beam flexure at the joint position achieved the best result. From the Finite-Element-Analysis result, we refined the flexure suspension by changing the dimension of the flexure pivots. The base flexure pivots were made relatively thicker and shorter while the remaining joints used long thin beam flexure pivots. Finally, we obtained an eight-bar flexure suspension shown in Fig.5.

In Finite-Element-Analysis, we applied aluminum as the material of the eight-bar flexure suspension. The base link of

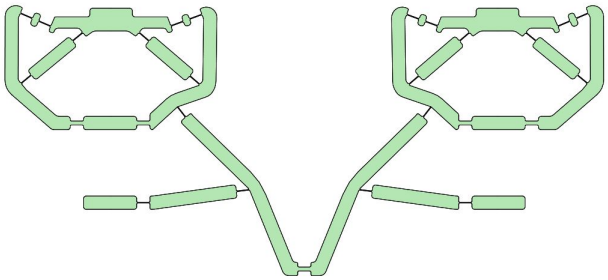

FIGURE 9. DESIGN OF THE DRIVING LINKAGE WITH HINGES REPLACED BY BEAM FLEXURES.

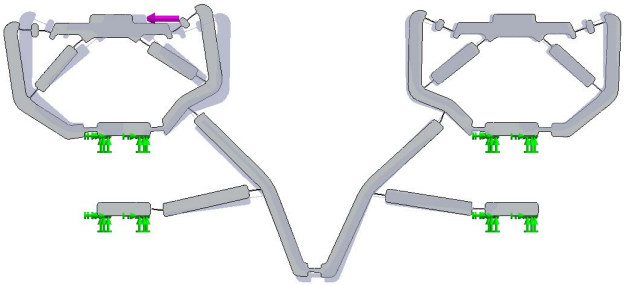

FIGURE 10. FINITE ELEMENT ANALYSIS SHOWING DISPLACEMENT OF THE DRIVING LINKAGE AND EIGHT-BAR FLEXURE SUSPENSION.

the whole flexure suspension was fixed and horizontal force was applied at the end-effector. We used a curvature based mesh. The stress result is shown in Fig.6. The highest stress was observed at the two flexure pivots besides the base link. The displacement result is shown in Fig.7. The motion of the eight-bar flexure suspension was very close to the rigid-body solution. From the Finite-Element-Analysis result we can see the eight-bar flexure suspension has well-performed rectilinear motion property.

MEMS GYROSCOPE

The technology we used in MEMS gyroscope fabrication required the minimum beam width to be 3 microns and the gap width is between 0.7 micron and 50 microns. We need to scale our design to fit the fabrication rules in order to manufacture it. Different fabrication technology has different constraints. One example can been seen from [3, 15].

A driving linkage was designed to connect two sets of MEMS gyroscopes. Trusov et al. (2011) [16] has presented the conventional coupling mechanism used in MEMS gyroscope.

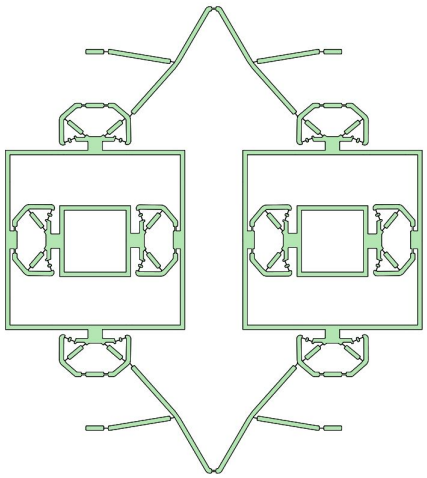

FIGURE 11. LAYOUT FOR A MEMS GYROSCOPE PROVIDING FLEXURES SUSPENSIONS OF THE PROOF MASS IN TWO DIMENSIONS.

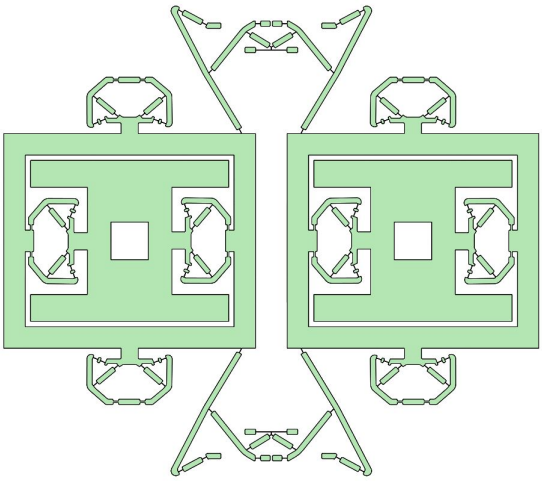

FIGURE 12. REVISED LAYOUT FOR A MEMS GYROSCOPE WITH A NEW DRIVING LINKAGE.

The driving linkage in our research was constructed from two Chebyshevs Lambda linkages. The end-effector of Chebyshevs Lambda mechanism can go through straight line within a specific range. Part of one bar from eight-bar linkage was used as one link of the Chebyshevs Lambda linkage. We connect the end-effector of the two Chebyshevs Lambda linkages together to get our driving linkage. The model of the driving linkage connecting two eight-bar linkages is shown in Fig.8. The input was applied at the end-effector of the Chebyshevs Lambda linkage. Because of the rectilinear motion of the Chebyshevs Lambda linkages, the two eight-bar linkages can be driven to move in opposite directions,

at the same time. An important MEMS gyroscope design rule is for small input to result in a large output so the driving linkage has to be made with high precision to achieve this goal. We transferred the rigid-body driving linkage to flexure pivots version as shown in Fig.9. Finite-Element-Analysis was conducted on evaluating the performance of the driving linkage. The displacement result is shown in Fig.10. We can see the two eight-bar flexure suspension moved in straight line validating the flexure pivots driving linkage performance.

CURRENT DESIGN

The long thin beam flexure pivots worked effectively in our current research. The whole MEMS gyroscope package included two sets of suspension connected by the driving linkage. Two examples of our current package design are shown in Fig.11 and Fig.12.

CONCLUSION

In this paper, we present a symmetric flexure-connected eight-bar linkage designed to be a rectilinear suspension for the proof mass of a MEMS gyroscope. This rectilinear eight-bar linkage was designed with hinged pivots and then flexures were introduced and sized using Finite Element Analysis. The result is an eight-bar flexure suspension that provides 33 micrometers of travel end-to-end with a maximum 0.1% deviation of the end-effector path from a straight line.

Additional work will be to adjust the symmetric eight-bar flexure suspension to meet fabrication rules and verifying that the finished product achieves the predicted rectilinear properties. Fabrication of prototypes will verify the motion of this flexure-connected eight-bar linkage under the action of external forces. Further research and experimentation will be conducted to refine the design of this rectilinear MEMS suspension.

ACKNOWLEDGMENT

The authors gratefully acknowledge the support of the National Science Foundation award CMMI-1066082. Any opinions, findings, and conclusions or recommendations expressed in this material are those of the authors, and do not necessarily reflect the views of the National Science Foundation.

REFERENCES

[1] Pham, Huy Hoang, and I-Ming Chen, "Kinematics, workspace and static analyses of 2-DOF flexure parallel mechanism," *Control, Automation, Robotics and Vision, 2002, ICARCV 2002, 7th International Conference on* Vol. 2. IEEE, 2002.

[2] Shi, Qin, Shourong Wang, Anping Qiu, Yishen Xu, and Xunsheng Ji, "Design principle of suspension of MEMS gyroscope," *Nano/Micro Engineered and Molecular Systems, 2006, NEMS'06, 1st IEEE International Conference on* IEEE, 2006.

[3] Alper, Said Emre, and Tayfun Akin, "A single-crystal silicon symmetrical and decoupled MEMS gyroscope on an insulating substrate," *Microelectromechanical Systems, Journal of* 14.4 (2005): 707-717.

[4] Kempe, Alfred Bray, *How to draw a straight line: a lecture on linkages,* Macmillan and Company, 1877.

[5] McCarthy, J. Michael, and Gim Song Soh, *Geometric design of linkages,* Vol. 11. Springer, 2010.

[6] Soh, G., and J. McCarthy, "Synthesis of Eight-Bar Linkages as Mechanically Constrained Parallel Robots," *12th IFToMM world congress A,* Vol. 653. 2007.

[7] Soh, Gim Song, and Fangtian Ying, "Dimensional Synthesis of Planar Eight-Bar Linkages Based on a Parallel Robot With a Prismatic Base Joint," *ASME 2013 International Design Engineering Technical Conferences and Computers and Information in Engineering Conference,* American Society of Mechanical Engineers, 2013.

[8] Chen, C., J. Angeles, and McGill Univerisity,"Kinematic synthesis of an eight-bar linkage to visit eleven poses exactly," *Proc. CDEN/C2E2 2007 Conference,* 2007.

[9] Sonawale, Kaustubh H., and J. Michael McCarthy, "Synthesis of Useful Eight-Bar Linkages as Constrained 6R Loops," *ASME 2014 International Design Engineering Technical Conferences and Computers and Information in Engineering Conference,* American Society of Mechanical Engineers, 2014.

[10] Kota, Sridhar, "Design of compliant mechanisms: Applications to MEMS," *1999 Symposium on Smart Structures and Materials,* International Society for Optics and Photonics, 1999.

[11] Avadhanula, Srinath, and Ronald S. Fearing, "Flexure design rules for carbon fiber microrobotic mechanisms," *Robotics and Automation, 2005, ICRA 2005, Proceedings of the 2005 IEEE International Conference on* IEEE, 2005.

[12] Howell, Larry L., and A. Midha, "A method for the design of compliant mechanisms with small-length flexural pivots," *Journal of Mechanical Design* 116.1 (1994): 280-290.

[13] Awtar, Shorya, Alexander H. Slocum, and Edip Sevincer "Characteristics of beam-based flexure modules," *Journal of Mechanical Design* 129.6 (2007): 625-639.

[14] Howell, L. L., and A. Midha, "Parametric deflection approximations for end-loaded, large-deflection beams in compliant mechanisms," *Journal of Mechanical Design* 117.1 (1995): 156-165.

[15] Xie, Huikai, and Gary K. Fedder, "Fabrication, characterization, and analysis of a DRIE CMOS-MEMS gyroscope,"

Sensors Journal, IEEE 3.5 (2003): 622-631.
[16] Trusov, Alexander A., et al, "Low-dissipation silicon tuning fork gyroscopes for rate and whole angle measurements," *Sensors Journal,* IEEE 11.11 (2011): 2763-2770.
[17] Geen et 31., "New iMEMS AngulariRateiSensing Gyroscope," *Analog Dialogue* 37-03, pp. 1-4 (2003).